Wave fronts and spatiotemporal chaos in an array of coupled Lorenz oscillators

Diego Pazó,* Noelia Montejo, and Vicente Pérez-Muñuzuri
Grupo de Física no Lineal, Facultad de Física, Universidad de Santiago de Compostela, 15706 Santiago de Compostela, Spain
(Received 19 October 2000; revised manuscript received 1 March 2001; published 15 May 2001)

The effects of coupling strength and single-cell dynamics (SCD) on spatiotemporal pattern formation are studied in an array of Lorenz oscillators. Different spatiotemporal structures (stationary patterns, propagating wave fronts, short wavelength bifurcation) arise for bistable SCD, and two well differentiated types of spatiotemporal chaos for chaotic SCD (in correspondence with the transition from stationary patterns to propagating fronts). Wave-front propagation in the bistable regime is studied in terms of global bifurcation theory, while a short wavelength pattern region emerges through a pitchfork bifurcation.

DOI: 10.1103/PhysRevE.63.066206 PACS number(s): 05.45.Xt, 45.70.Qj

I. INTRODUCTION

The study of networks of coupled systems is an interesting issue from both mathematical and applied physics points of view. In this paper, we focus on a one-dimensional array of systems such that each cell evolves in time according to an ordinary differential equation (ODE). Assemblies of this kind are known as *lattice dynamical systems* (LDS's). The simplification arises from the fact that units are described just by ODE's, so the field of application is significantly wide: lasers [1], neural systems [2], Josephson junctions [3,4], reaction-diffusion systems [5], and electronic oscillators [6,7], among others. LDS's are relevant not only in physics, but also in biology. Paradigmatic examples are the Nagumo [8] and the FitzHugh-Nagumo [9] models, where the dynamics of a single unit is described by one and two variables, respectively. Phenomena such as the propagation of traveling wave fronts have been studied from a mathematical point of view [10–14].

However, cases where the dynamics of a single cell within an array is described by two or more variables have aroused a great deal of interest in recent years. Here pattern formation arising in bistable systems can show interesting properties [15], and if the array consists of a certain number of coupled chaotic oscillators complex behaviors, such as nontrivial collective behavior [16], size instability [17], rotating waves [18,19] or partial synchronization [20] can develop. What behaviors may be expected and what exactly is the role of the coupling strength are just two of the unsettled questions. Here we try to gain some insight into these problems.

In this paper, we study an array made up of identical units. The coupling among them is of diffusive type (i.e., bidirectional),

$$\dot{\mathbf{r}}_j = f(\mathbf{r}_j) + \frac{D}{2}\Gamma(\mathbf{r}_{j+1} + \mathbf{r}_{j-1} - 2\mathbf{r}_j), \tag{1}$$

where $\mathbf{r}_j \in \mathbb{R}^n$. D is the coupling parameter, and Γ is the coupling matrix. Although the case $n=1$ has been studied extensively, there exists a large gap referring to greater dimensions ($n>1$).

II. MODEL

The type of function f in Eq. (1), the coupling strength D, and the coupling matrix Γ determine the dynamics of the whole array. Due to its well studied phase space and its richness of behaviors, we deal with the Lorenz oscillator as a unit cell ($n=3$). In particular, we focus on the bistable region and the transition to the chaotic region. Arrays consisting of Lorenz oscillators connected through a local, nearest neighbor coupling have been considered in recent works [15,21,22].

In what concerns the type of coupling matrix, several situations seem to be quite natural. These are the cases where all the elements of Γ are zero except one (that we take to be equal to 1). The case $\Gamma = I$ has been studied very recently [21,22]. Three situations are of special interest as long as they present front propagation (this phenomenon will be explained in detail below):

$$\Gamma = \begin{pmatrix} 0 & 1 & 0 \\ 0 & 0 & 0 \\ 0 & 0 & 0 \end{pmatrix}, \quad \begin{pmatrix} 0 & 0 & 0 \\ 1 & 0 & 0 \\ 0 & 0 & 0 \end{pmatrix}, \quad \begin{pmatrix} 0 & 0 & 0 \\ 0 & 1 & 0 \\ 0 & 0 & 0 \end{pmatrix}. \tag{2}$$

For the rest of the coupling matrices, the identity matrix or matrices with one element different from zero, no front propagation has been obtained numerically [23]. We decided to focus on the first coupling matrix in Eq. (2) since in this case, as will be shown later, the system undergoes a short wavelength bifurcation which enriches the kind and number of patterns described later.

Thus our dynamical equations are

$$\begin{aligned} \dot{x}_j &= \sigma(y_j - x_j) + \frac{D}{2}(y_{j+1} + y_{j-1} - 2y_j), \\ \dot{y}_j &= r x_j - x_j z_j - y_j, \quad j = 1, \ldots, N \\ \dot{z}_j &= x_j y_j - b z_j . \end{aligned} \tag{3}$$

*Email address: diego@fmmeteo.usc.es; http://chaos.usc.es

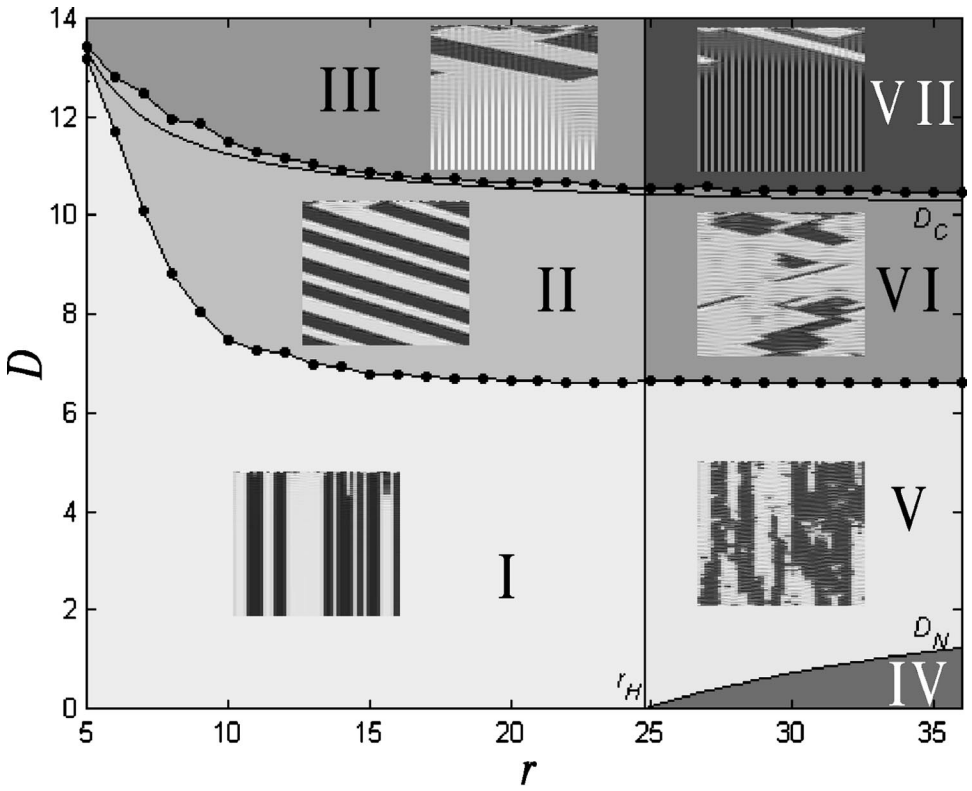

FIG. 1. Phase space of the patterns obtained for an array of coupled Lorenz oscillators. Left regions correspond to $r<r_H$ where the Lorenz oscillator is bistable, and right regions correspond to $r>r_H$ where the Lorenz oscillator is chaotic. A representative temporal evolution of a ring is located for each zone. They display, in gray scale, the x coordinate vs time that runs downward; initial conditions are random. Each region corresponds to a different characteristic dynamics. Region I: multistability (i.e., spatial chaos). Region II: front propagation. Region III: short-wavelength ordering. Region V: spatiotemporal chaos. Region VI: spatiotemporal chaos with front propagation. Region VII: short-wavelength ordering with transient chaos. Region IV: spatiotemporal chaos without clusters. Solid lines correspond to theoretical results D_C and D_N [Eqs. (6) and (7), respectively].

Off-diagonal diffusive-type coupling appears in mechanical models with elastic junctions, like the stick-slip Burridge-Knopoff model (see, e.g., Ref. [24], and references therein). Moreover, in terms of an electronic caricature, this coupling represents an active transmission line where cells are coupled through capacitances and inductances.

Both periodic and null-flow boundary conditions are used. The parameters σ and b are fixed at the values $\sigma=10$ and $b=8/3$. The other relevant parameter besides the coupling strength D is r, that controls the internal state (chaotic or bistable) of the oscillators. For the dynamics of a single unit, there exists a critical value

$$r_H=\frac{\sigma(\sigma+b+3)}{\sigma-b-1}, \tag{4}$$

which for the given values of σ and b is $r_H\approx 24.74$. For $1<r<r_H$ the units are bistable, with two symmetric stable fixed points $C_\pm=[\pm\sqrt{b(r-1)},\pm\sqrt{b(r-1)},r-1]$ and one unstable fixed point at the origin. For $r>r_H$ all the fixed points are unstable and the unit exhibits the well known Lorenz strange attractor.

A fourth-order Runge-Kutta method was used to integrate Eq. (3). A diagram of the patterns obtained by varying D and r is shown in Fig. 1. We analyze the bistable region in Sec. III, and the chaotic one in Sec. IV.

III. BISTABLE REGION

As mentioned above, the single-unit fixed points $C_\pm$ are stable in the range $(1, r_H)$. Therefore, the whole system is multistable in that range [25] for $D=0$.

A. Traveling fronts

Traveling front propagation has been a long-term field of research. Restricting ourselves to the bistable case, there are two paradigmatic examples: the Nagumo and FitzHugh-Nagumo equations. Classically, fronts connect a pair of stable fixed points and propagate, driving the system toward its most stable state. Consider, for example, one-variable cells, namely, $\dot{u}_n=f(u_n)+D(u_{n+1}+u_{n-1}-2u_n)$. Then propagation will only succeed if $\int f(u)du\neq 0$. Furthermore, it does not occur until D is larger than a critical value D_{th}. Because of the discreteness of the system, $D_{th}>0$, while $D_{th}=0$ for the continuous version. The existence of a threshold for the discrete systems is called ''propagation failure'' [10].

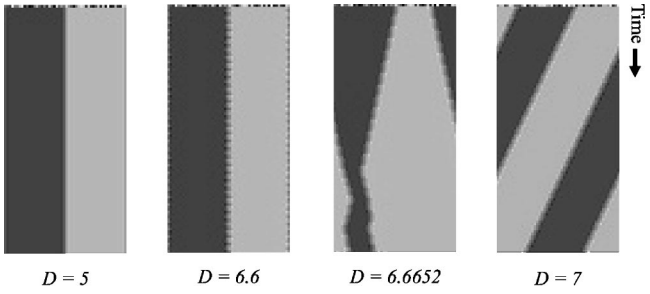

FIG. 2. A steplike initial condition is imposed for a ring of $N=50$ oscillators ($r=20$): $\mathbf{r}_i \approx C_+, i=1,\ldots,25$ and $\mathbf{r}_j \approx C_-, j=26,\ldots,50$. The value of the variable x is represented in gray scale. For high enough D, fronts start to propagate. Just on the threshold ($D_{th}=6.6652$) the system is not able to propagate fronts without undergoing spontaneous reversals. Just above the threshold the propagation does not change its sense spontaneously. In the case shown here, both fronts move in the same sense, giving a stable traveling-wave solution; if both fronts propagate in opposite senses, the whole ring will collapse to C_+ or C_-.

Propagation in continuous bistable systems has been extensively studied in Ref. [26]; showing that propagation is possible in *symmetric nongradient* reaction-diffusion systems. It is known that a transition from a static front to a propagating front involves a symmetry breaking of the front [26] through a pitchfork bifurcation. Here we show an apparently new way to break symmetry and, therefore, to achieve propagation for the discrete case. For the Lorenz oscillator, we have *symmetry* under the transformation $(x,y,z)\rightarrow(-x,-y,z)$, implying two stable *symmetric* fixed points ($C_\pm$). Beyond a critical value D_{th}, fronts can propagate in both senses with the same probability (because of the symmetry of the equations). Discreteness has traditionally been considered as a propagation inhibitor, but it is just the discreteness that now provides a route for propagation.

In Fig. 2 the effect of varying D for our bistable single cell dynamics is depicted. The transition to the propagating solution is as follows: as the coefficient D is increased, boundaries between domains of both solutions (C_+ and C_-) become smoother than the steplike boundary observed for $D=0$. That is, some oscillators move to the vicinity of C_+ and C_-. At a given value of D the boundaries start to oscillate, i.e., they undergo a Hopf bifurcation, but they do not propagate (see $D=6.6$ in Fig. 2), until finally, over a threshold D_{th}, propagation occurs. If the array is open (null-flow boundary condition), the whole system finally collapses to one of the two stable solutions. On the other hand, for the case of a ring (periodic boundary condition), stationary traveling wave-front solutions can be found.

In order to obtain a more precise knowledge of the bifurcation arising in the system, in Fig. 3 we represent the projection, onto the plane x-y, of the trajectory followed by all the oscillators of the array. For $D=0$, oscillators are in a steplike configuration; as D increases, a few cells in the neighborhood of the border of the steplike initial condition go to nearby points to C_+ and C_-. At $D\approx 6.92$ the symmetry of the system is broken through a pitchfork bifurcation, and is recovered when one of the oscillators reaches the origin at $D\approx 6.95$. At $D\approx 7.5$ the stationary front solution becomes unstable through a supercritical Hopf bifurcation. This corresponds to the point where the boundary between both domains begins to oscillate (see Fig. 2). The amplitude of the oscillations grows with D. Finally, for $D=D_{th}\approx 8.85$, the orbit of each oscillator collides with the orbits of its neighbors [27]. This collision originates a multiple heteroclinic connection. If the system is infinite, in terms of global coordinates, the situation can be reduced to a pair of symmetry related homoclinic connections in a periodic phase space. This situation is similar to the pendulum problem, where a set of separatrices (two in a cylindrical phase space) divide the phase space into several characteristic dynamics (libration and two opposite senses of rotation). Thus, in the last

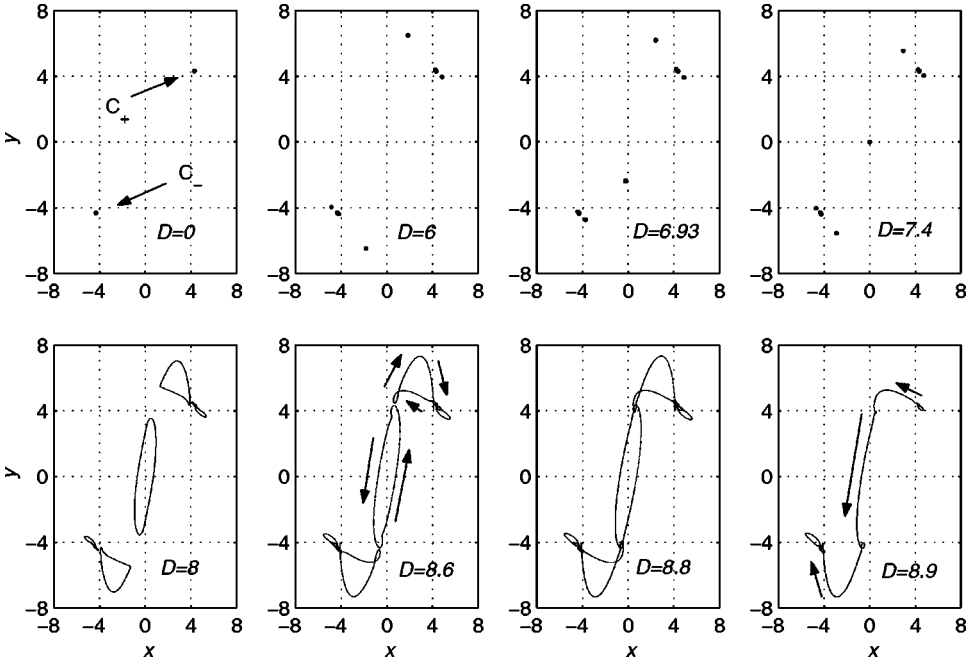

FIG. 3. Transition to propagation of a front from the trivial solution at $D=0$ as D increases. A projection onto the x-y plane of the trajectory, followed by the oscillators of the array, is shown for $r=8$ and different values of the coupling strength D. For $0<D<6{,}92$ the system is odd symmetric in the x-y plane. For $D\approx 6.92$ this symmetry is broken through a pitchfork bifurcation, but is recovered again for $D\approx 6.95$. At $D\approx 7.55$ the system undergoes a supercritical Hopf bifurcation, so that the front starts to oscillate. A further increase of D enlarges the orbit of each oscillator. Finally, for $D\approx 8.85$, all the orbits collide with their neighbor orbits. For a larger D, propagation occurs.

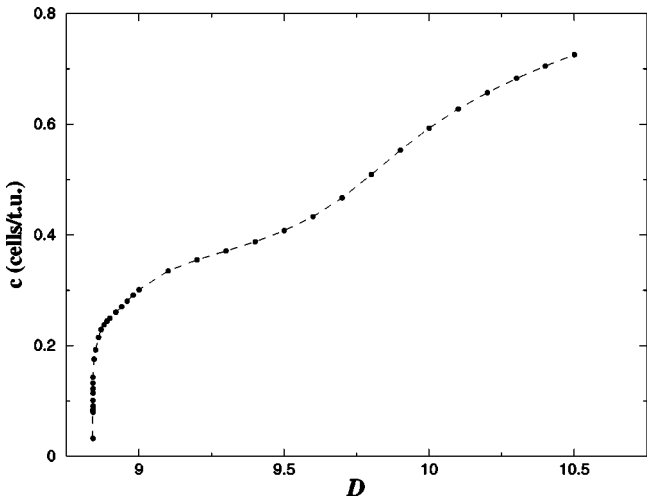

FIG. 4. Front propagation speed (c) as a function of the coupling strength D for $r=8$. t.u. (time units).

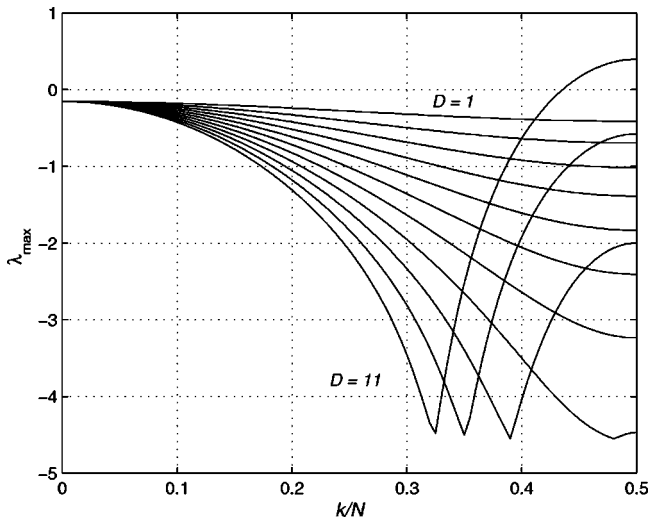

FIG. 5. Maximum eigenvalues at the uniform states in $C_{\pm}$ as a function of k for $D=1,2,\ldots,11$ and $r=20$.

picture of Fig. 3, when propagation occurs the oscillators follow a trajectory from C_+ to C_-, close to the set of heteroclinic orbits. The opposite solution (from C_- to C_+) is also possible, and is odd symmetric compared to the one displayed in Fig. 3.

The front velocity c, near the onset, arising from this route does not follow a square root law with $D-D_{th}$, as is usually found for other systems (see Fig. 4); instead it shows an inflection point for middle values of D, and near the threshold value c grows abruptly. In Ref. [28] the author found a system (for $n=1$) that belongs to a different universality class, but propagation occurs only in the presence of *asymmetry*. A detailed analysis of the front velocity for the route explained above will be published elsewhere.

B. Short-wavelength bifurcation

The trivial solutions $\mathbf{r}_1=\mathbf{r}_2=\cdots=\mathbf{r}_N=C_{\pm}$ are stable up to a critical value of the coupling parameter D. For this value, a short-wavelength bifurcation arises (see Fig. 1), and a stationary pattern (*zigzag*) develops consisting of an alternate sequence of cells in the vicinity of C_+ (or C_-). This pattern can coexist for some time with front propagation, and, in this case, at both sides of the wave front, for each domain, the zigzag pattern has been observed.

For a ring, the observed critical value fits very well with that calculated (D_C) from a linear stability analysis of the Fourier modes around any of the fixed points $C_{\pm}$. The secular equation for the Fourier modes (η_k) is

$$\dot{\eta}_k = S(k)\,\eta_k,$$

$$S(k)=\begin{pmatrix} -\sigma & \sigma-2D\sin^2\left(\dfrac{\pi k}{N}\right) & 0 \\ 1 & -1 & \mp\overline{c} \\ \pm\overline{c} & \pm\overline{c} & -b \end{pmatrix}, \tag{5}$$

where $\overline{c}=\sqrt{b(r-1)}$. The real part of the most unstable eigenvalue is plotted in Fig. 5 as a function of k for different values of D. For $k=0$ the stability is independent of D, and the fixed point is a spiral sink (because the less attracting eigenvalues are complex conjugates). However, for a large enough value of D, the shortest wavelength Fourier modes ($k\approx N/2$) are governed by the real eigenvalue. The maximum value of this eigenvalue is at $k=N/2$ (shortest wavelength), and crosses zero at $D=D_C$. At this point, the determinant of the Jacobian matrix $S(k=N/2)$ is zero. This condition gives the value of D_C:

$$D_C=\sigma\frac{r-1}{r-2}. \tag{6}$$

The result for an open array is the same as that for a ring up to $O(1/N^2)$. Above this critical value other modes become unstable, and the dynamics turns out to be more complex than the one shown in the top pictures of Fig. 1.

IV. CHAOTIC REGION

At $r=r_H$ the single unit fixed points $C_{\pm}$ become unstable through a subcritical Hopf bifurcation. The behavior of an isolated Lorenz oscillator then becomes chaotic for $r\geqslant r_H$. The system does not possess any stationary or periodic stable state.

For $D=0$ the oscillators are uncoupled, and the whole system is highly chaotic. The situation persists for low values of D. Finally, as the coupling increases, the system tends to form clusters around C_+ and C_-. The development of clusters occurs in a very smooth way; hence a precise limit cannot be assigned to such transition. An analytical calculation shows the tendency toward cluster formation as r grows. The latter proceeds through calculations of the eigenvalues of the system at the uniform state (all the oscillators are in the same fixed point). We first note that at $D=0$ all Fourier modes are unstable (assuming $r>r_H$). But, as long as D increases enough, there is a Fourier mode that becomes stable. This mode is $k=N/2$ (the shortest wavelength mode); the fact that this mode becomes stable causes the dynamics

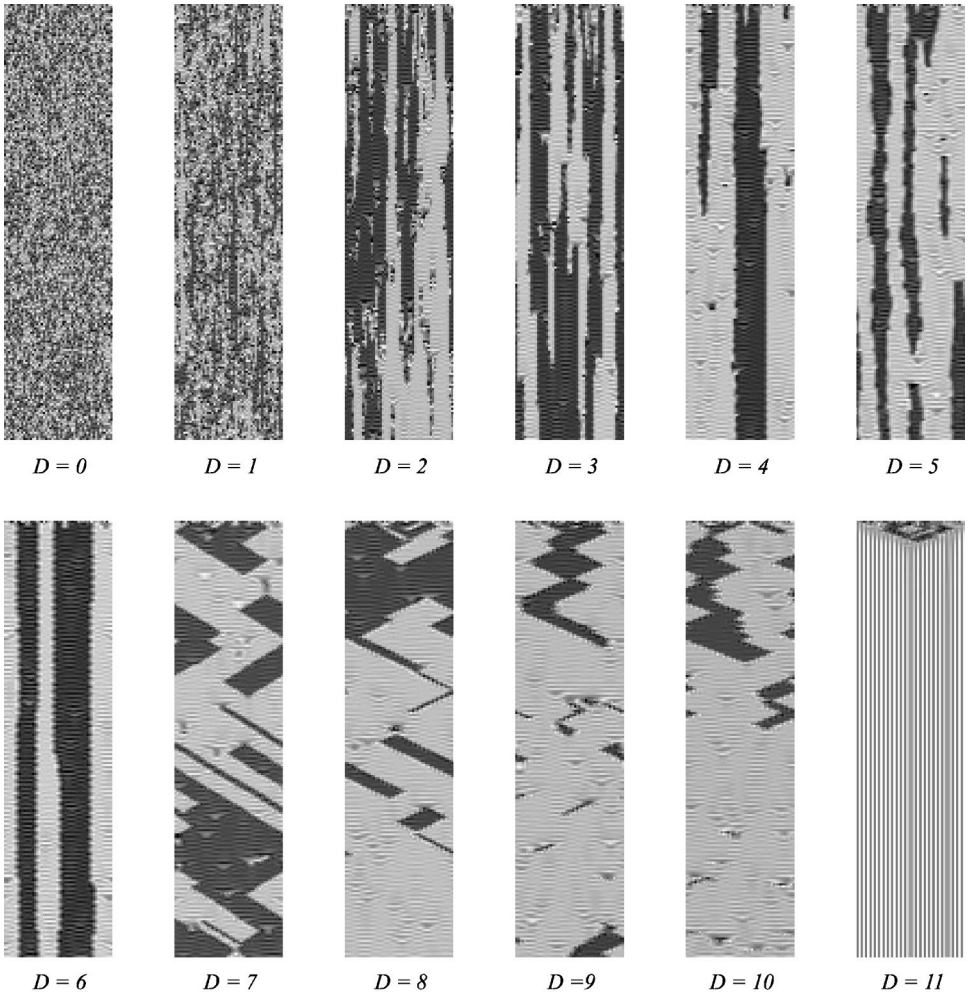

FIG. 6. Different behaviors for several couplings (D) for $r=28$ (the same initial condition was imposed in all cases). The behavior of the system changes drastically at two values of D. One point separates propagation and no propagation of fronts, and is located between $D=6$ and 7. The second point separates the zone where short-wavelength bifurcation arises, and is located just above $D=\sigma=10$. In the picture corresponding to $D=11$, the system suffers a short-wavelength bifurcation with two dislocations (located at the center and at the right-hand side).

of neighboring oscillators to diverge less strongly than before; this can be considered as the beginning of cluster formation. The value of D corresponding to this point is a function of r:

$$D_N=\frac{(\sigma+1+b)b(\sigma+r)-2\sigma b(r-1)}{2[\sigma+1+b(3-r)]}. \tag{7}$$

The corresponding curve is shown in Fig. 1. On the other hand, the maximum transverse Lyapunov exponents $\lambda_{k\geq 1}$ of each mode η_k, calculated around the chaotic synchronized state (see, e.g., Ref. [29]), show a dependence on D equivalent to the behavior of the Lyapunov exponents at the fixed points, but the mode $k=N/2$ becomes stable at a larger value of D. The system ''prefers'' to form clusters around fixed points rather than forming an extended coherent structure (consisting for example of some cells of the array partially synchronized) with the Lorenz chaotic attractor as the basis for each cell dynamics. Since our clusters are defined as long-lasting ensemble of cells close to C_+ or C_-, transverse Lyapunov exponents around the chaotic synchronized state do not give any new information.

At higher values of D, for which traveling waves appeared for $r<r_H$, now the array forms clusters whose boundaries propagate as traveling waves (see Figs. 1 and 6). Because of the instability of the fixed points, front reversals are observed, as is the spontaneous formation of new clusters through the appearance of two counter propagating fronts. The formation of new clusters becomes more frequent as r grows. So, for r just above r_H, the whole array is maintained for a long time, with all the oscillators turning around one of the fixed points (either C_+ or C_-), until two counterpropagating fronts are able to emerge. Recall that, independently of the initial conditions, the onset of traveling fronts makes the system collapse around C_+ or C_-. For this situation, the phase (ϕ) and amplitude (A) can be properly defined [30] by means of the projection shown in Fig. 7. We chose to define phase and amplitude as follows [31]:

$$\phi=\arctan\left(\frac{\sqrt{x^2+y^2}-\sqrt{2b(r-1)}}{z-(r-1)}\right), \tag{8}$$

$$A^2=[|x|-\sqrt{b(r-1)}]^2+[|y|-\sqrt{b(r-1)}]^2+[z-(r-1)]^2. \tag{9}$$

There are domains where the phase of the neighbor oscillators is highly correlated (see Fig. 8). The limits of these domains are oscillators whose amplitude is zero or close to zero, and could be considered as defects (in analogy with the

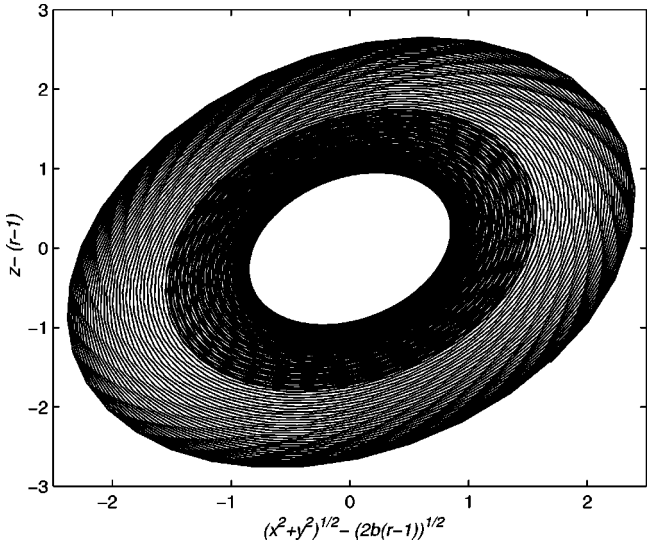

FIG. 7. Dynamics of one oscillator for $D=8$ and $r=25$ in a reference framework where phase can be readily computed.

Ginzburg-Landau (GL) equation phenomenology). The subcritical Hopf bifurcation observed in the Lorenz oscillator does not involve a pair of stable limit cycles (one for C_+, and another for C_-). There is not a range of values of r where the system presents multistability between a limit cycle and a fixed point [32,33]. Therefore, the transition observed in the array cannot be considered simply as a discretized subcritical GL transition in C_+ or C_- [34,35].

Finally, it must be pointed out that, as r grows, the fixed points $C_\pm$ become more and more unstable. As a consequence, cluster sizes become smaller, and eventually it is not possible to distinguish between nonpropagating and propagating regions.

With respect to the short-wavelength bifurcation arising in the bistable region, this structure remains stable beyond r_H. The (Hopf) instability of $C_\pm$ does not affect the zigzag structures bifurcated from the uniform solutions. An analytical calculation of the stability of these patterns is not feasible, because the solutions depend on both r and D. However, we can argue that the result obtained in Eq. (6) can be extended successfully to the chaotic region (Fig. 1). In this region the mode $k=0$ is unstable, and as r increases further from r_H some long wavelength modes ($k=1,2,\ldots$) also become unstable. So, in this zone, the problem is harder to treat than in the bistable zone, because there is more than one unstable mode. The dynamics of the system is determined by the behavior of each Fourier mode. Whereas $k=0$ is unstable (independently of D), long-wavelength modes stabilize as D increases. On the other hand, short-wavelength modes become stable for low D but turn unstable again when D approaches D_C. Therefore, the shortest-wavelength modes govern the dynamics at high values of D. Due to the chaotic dynamics existing for $r>r_H$, the system is eventually close enough to one of the uniform solutions, and then is shifted to one of the frozen zigzag patterns.

V. CONCLUSIONS

This paper studies an array of oscillators where wavefront solutions arise. Starting from the uncoupled case, when

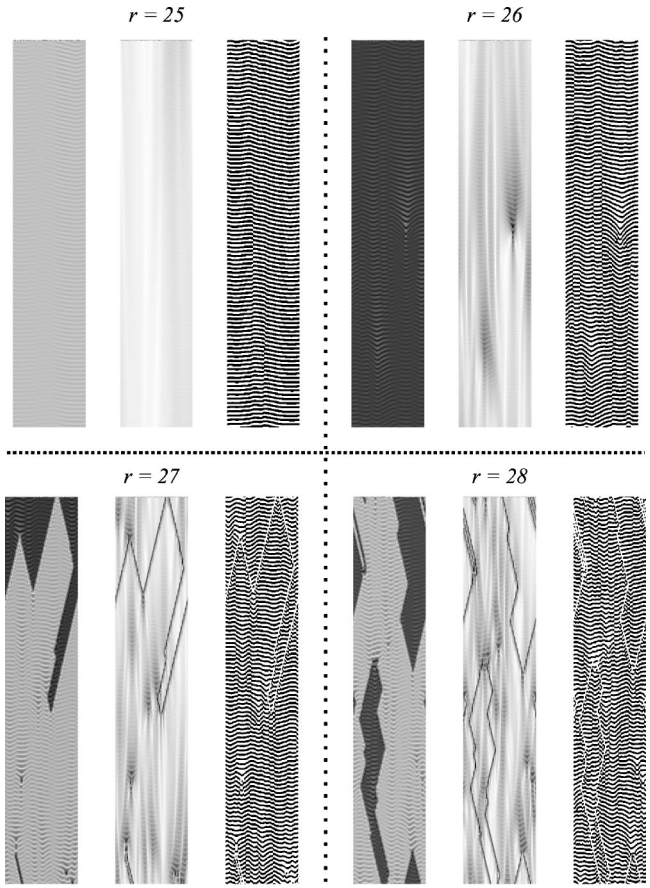

FIG. 8. The system for $D=8$ and $r=25$, 26, 27, and 28. Each value of r shows three pictures, from left to right: x variable, amplitude, and two-color-discretized phase. As long as r increases the phase correlation diminishes, because of the appearance of more fronts and defects (small amplitude, i.e., white color).

D reaches a critical value fronts start to oscillate due to the onset of a supercritical Hopf bifurcation. When D is increased further, the amplitude of the oscillations grows until two symmetry related heteroclinic connections appear. A further increasing of D causes propagation of the fronts. For this kind of route to front propagation, wave velocity was not found to follow a square root law with $D-D_{th}$. Moreover, it seems that this route to propagation needs of units whose dimension is two or more. The Hopf bifurcation is an essential ingredient, and each unit needs a two-dimensional manifold to oscillate.

Furthermore, it has been shown that once the fixed points become unstable for $D<D_C$, the system exhibits two types of spatiotemporal chaos depending on whether front propagation exists or not. In the propagating region we find two characteristic processes: spontaneous creation of counterpropagating fronts and front reversal. The boundary that separated propagating and nonpropagating regions in the bistable case now separates these two kinds of spatiotemporal chaos.

We have also found that over a certain coupling the system undergoes a *short-wavelength bifurcation*. This kind of bifurcation is observed in discrete systems only; we also ob-

served the onset of propagating fronts by the route explained above. We have also observed that this short-wavelength pattern inhibits the spatiotemporal chaos beyond r_H, giving rise to an ordered pattern. All the necessary conditions to achieve the behaviors described above are still a matter of future research.

ACKNOWLEDGMENTS

We want to thank Roberto Deza by his very valuable comments in the preparation of the manuscript. The support by DGES and MCyT under Research Grant Nos. PB97–0540 and BFM2000-0348 is gratefully acknowledged.

[1] R.D. Li and T. Erneux, Phys. Rev. A **49**, 1301 (1994).
[2] H.D.I. Abarbanel, M.I. Rabinovich, A. Selverston, M.V. Bazhenov, R. Huerta, M.M. Sushchik, and L.L. Rubchinskii, Usp. Fiz. Nauk **166**, 1 (1996) [Phys. Usp. **39**, 337 (1996)].
[3] S. Nichols and K. Wiesenfeld, Phys. Rev. E **50**, 205 (1994).
[4] S. Watanabe, S.H. Strogatz, H.S.J. van der Zant, and T.P. Orlando, Phys. Rev. Lett. **74**, 379 (1995).
[5] T. Erneux and G. Nicolis, Physica D **67**, 237 (1993).
[6] V. Pérez-Muñuzuri, V. Pérez-Villar, and L.O. Chua, Int. J. Bifurcation Chaos Appl. Sci. Eng. **2**, 403 (1992).
[7] A.P. Muñuzuri, V. Pérez-Muñuzuri, M. Gómez-Gesteira, L.O. Chua, and V. Pérez-Villar, Int. J. Bifurcation Chaos Appl. Sci. Eng. **5**, 17 (1995).
[8] H.P. McKean, Adv. Math. **4**, 209 (1970).
[9] R. FitzHugh, Biophys. J. **1**, 445 (1961).
[10] J.P. Keener, SIAM (Soc. Ind. Appl. Math.) J. Appl. Math. **47**, 556 (1987).
[11] B. Ziner, SIAM (Soc. Ind. Appl. Math.) J. Math. Anal. **22**, 1016 (1991).
[12] D. Hankerson and B. Ziner, J. Dyn. Diff. Eq. **5**, 359 (1993).
[13] S.-N. Chow and W. Shen, SIAM (Soc. Ind. Appl. Math.) J. Appl. Math. **55**, 1764 (1995).
[14] R.S. MacKay and J.-A. Sepulchre, Physica D **82**, 243 (1995).
[15] K. Josić and E. Wayne, J. Stat. Phys. **98**, 1 (2000).
[16] M.C. Cross and P.C. Hohenberg, Rev. Mod. Phys. **65**, 851 (1993).
[17] J.F. Heagy, L.M. Pecora, and T.L. Carroll, Phys. Rev. Lett. **74**, 4185 (1995).
[18] M.A. Matías, J. Güémez, V. Pérez-Muñuzuri, I.P. Mariño, M.N. Lorenzo, and V. Pérez-Villar, Europhys. Lett. **37**, 379 (1997).
[19] D. Pazó, I.P. Mariño, V. Pérez-Villar, and V. Pérez-Muñuzuri, Int. J. Bifurcation Chaos Appl. Sci. Eng. **10**, 2533 (2000).
[20] R. Huerta, M. Bazhenov, and M.I. Rabinovich, Europhys. Lett. **43**, 719 (1998).
[21] N.J. Balmforth, C. Pasquero, and A. Provenzale, Physica D **138**, 1 (2000).
[22] H.-K. Park and H.-T. Moon (unpublished).
[23] Calculations were performed for the values of parameters σ and b used in Eq. (3), and $r \in (5,36)$.
[24] J.H.E. Cartwright, E. Hernández-García, and O. Piro, Phys. Rev. Lett. **79**, 527 (1997).
[25] For values of r smaller than, but very close to, r_H, the chaotic attractor coexists with the fixed points $C_\pm$, but this is of minor importance here.
[26] A. Hagberg and E. Meron, Nonlinearity **7**, 805 (1994).
[27] We have measured such distances, observing that the distances between neighboring orbits really fall to zero for $D = D_{th}$.
[28] G. Fáth, Physica D **116**, 176 (1998).
[29] M. Zhan, G. Hu, and J. Yang, Phys. Rev. E **62**, 2963 (2000).
[30] A. Pikovsky, M. Rosenblum, G. Osipov, and J. Kurths, Physica D **104**, 219 (1997).
[31] A stricter way to define ϕ and A would be to pass to the two-dimensional manifold, where the subcrirical Hopf bifurcation takes place. In this two-dimensional manifold a Ginzburg-Landau (GL) equation should be found in such a way that ϕ and A are strictly defined. Nonetheless, our definitions are one to one related with those whose definition came from the GL equation. Furthermore, it would be intriguing how to cast a definition valid for C_+ and C_-. Hence the important features of the dynamics will be readily provided by our operational definitions.
[32] A.-D. Defontaines and Y. Pomeau, Physica D **46**, 201 (1990).
[33] V.I. Nekorkin, V.A. Makarov, and M.G. Velarde, Int. J. Bifurcation Chaos Appl. Sci. Eng. **6**, 1845 (1996).
[34] S. Fauve and O. Thual, Phys. Rev. Lett. **64**, 282 (1990).
[35] W. van Saarloos and P.C. Hohenberg, Phys. Rev. Lett. **64**, 749 (1990).